

Accepted Manuscript

Title: In-depth rheological characterization of genetically modified xanthan-variants

Authors: Moritz Gansbiller, Jochen Schmid, Volker Sieber

PII: S0144-8617(19)30197-3
DOI: <https://doi.org/10.1016/j.carbpol.2019.02.055>
Reference: CARP 14628



To appear in:

Received date: 5 November 2018
Revised date: 15 February 2019
Accepted date: 16 February 2019

Please cite this article as: Gansbiller M, Schmid J, Sieber V, In-depth rheological characterization of genetically modified xanthan-variants, *Carbohydrate Polymers* (2019), <https://doi.org/10.1016/j.carbpol.2019.02.055>

This is a PDF file of an unedited manuscript that has been accepted for publication. As a service to our customers we are providing this early version of the manuscript. The manuscript will undergo copyediting, typesetting, and review of the resulting proof before it is published in its final form. Please note that during the production process errors may be discovered which could affect the content, and all legal disclaimers that apply to the journal pertain.

In-depth rheological characterization of genetically modified xanthan-variants

Moritz Gansbiller^a, Jochen Schmid^{a,b} and Volker Sieber^{a,c,d,e*}

^a *Chair of Chemistry of Biogenic Resources, Technical University of Munich, Campus for Biotechnology and Sustainability, Schulgasse 16, 94315 Straubing, Germany*

^b *Chair of Bioprocess Engineering, Technical University of Munich, Campus for Biotechnology and Sustainability, Schulgasse 16, 94315 Straubing, Germany*

^c *Fraunhofer IGB, Straubing Branch BioCat, Schulgasse 23, 94315 Straubing, Germany*

^d *TUM Catalysis Research Center, Ernst-Otto-Fischer-Straße 1, 85748 Garching, Germany*

^e *The University of Queensland, School of Chemistry and Molecular Biosciences, 68 Copper Road, St. Lucia 4072, Australia*

Authors:

Moritz Gansbiller: m.gansbiller@tum.de

Jochen Schmid: j.schmid@tum.de

Volker Sieber: sieber@tum.de

*** Corresponding author**

Prof. Dr. Volker Sieber

Chair of Chemistry of Biogenic Resources

Technical University of Munich

Schulgasse 16

94315 Straubing, Germany

Tel: +499421/187300

Fax: +499421/187310

sieber@tum.de

Highlights

- First thorough rheological characterization of in-vivo engineered xanthan variants
- Higher impact of pyruvylation than acetylation on rheological properties of xanthan
- Position of acetylation affects rheological properties of xanthan
- Acetylation of xanthan plays significant role in thermostability of its rheological properties

Abstract

Xanthan is an extensively studied viscosifying agent discovered in 1961. Acetylation and pyruvylation have a major influence on its rheological properties and the effect of these groups on the conformation and rheological properties of xanthan have been studied for decades. However, these studies rely mainly on chemical modifications and therefore the degree of pyruvylation and acetylation as well as regioselectivity of deacetylation cannot be controlled. Here, we present an in-depth rheological characterization of natural xanthan and seven xanthan-variants, with defined acetylation and pyruvylation patterns created via genetic modification of *Xanthomonas campestris* LMG 8031. By that approach xanthan-variants with defined acetylation and pyruvylation patterns in their most natural state due to the mild production conditions were obtained. It was possible to link the defined substituent patterns to their corresponding rheological properties to give novel structure-function relationship insights of xanthan-variants in salt-free environments and in the presence of mono- and divalent cations.

Keywords: xanthan; in-vivo engineering; rheology; acetylation; pyruvylation

1 Introduction

Xanthan, the exopolysaccharide produced by *Xanthomonas campestris* is one of the most commonly used microbial exopolysaccharides as a thickening agent for a wide range of industrial applications, due to its commercial availability (Becker, Katzen, Pühler, & Ielpi, 1998). Natural xanthan's field of application ranges from food, cosmetic and pharmaceutical products to construction and oil drilling industry (Palaniraj & Jayaraman, 2011). xanthan

biosynthesis follows the *Wzx/Wzy*-pathway (Schmid, Sieber, & Rehm, 2015) and the 12 involved genes *gumB-gumH* are arranged in the 16 kilobasepairs (kbp) *gum*-cluster (Katzen, Becker, Zorreguieta, Pühler, & Ielpi, 1996). The genes *gumD*, *-M*, *-H*, *-K* and *-I* are involved in the synthesis of the pentasaccharide repeating unit (Becker et al., 1998; Ielpi, Couso, & Dankert, 1981; Vorhölter, Schneiker, Goesmann, Krause, & Bekel, 2008), while the genes *gumB*, *-C*, *-E* and *-J* are involved in polymerization and export of the polysaccharide (Becker et al., 1998; Galvan et al., 2013; Ielpi et al., 1981; Vorhölter et al., 2008). The repeating unit of xanthan consists of two β -(1 \rightarrow 4) linked β -D-glucose (Glc) units as backbone and a trisaccharide sidechain, α -(1 \rightarrow 3)-linked to every other glucose. The sidechain is composed of α -D-mannose (Man), β -D-glucuronic acid (GlcA) and β -D-mannose (Man), which are β -(1 \rightarrow 2) and β -(1 \rightarrow 4) linked to another, respectively (Jansson, Kenne, & Lindberg, 1975). In its natural state the α -D-Man is acetylated by the acetyltransferase GumF and the β -D-Man is either acetylated or pyruvylated by the acetyltransferase GumG or pyruvate ketalase GumL, respectively (Jansson et al., 1975). The total amount of substituents highly depends on the used strain as well as culture conditions and can range from 6.5 % to 13 % for acetate and 2.8 % to 14 % for pyruvate (Abbaszadeh et al., 2015; Garcia-Ochoa, Santos, Casas, & Gomez, 2000; Li & Feke, 2015). While xanthan exhibits excellent thickening properties over a wide range of pH and temperature (Garcia-Ochoa et al., 2000), the influence of salts on its rheological behavior is remarkable and has been widely studied (Bergmann, Furth, & Mayer, 2008; Callet, Milas, & Rinaudo, 1987; Dário, Hortêncio, Sierakowski, Neto, & Petri, 2011; Galván et al., 2018; Xu, Dong, Gong, Sun, & Li, 2015). Because of the regioselectivity of the transferases, it is possible, to create xanthan-variants with specific acetylation and pyruvylation-patterns by deletions of the genes *gumF*, *gumG* and *gumL* and combinations thereof. Although there have been recent studies about the impact of acetylation and pyruvylation of xanthan on its physicochemical properties (Khouryieh, Herald, Aramouni, Bean, & Alavi, 2007; Kool, Gruppen, Sworn, & Schols, 2013, 2014; Kool, Schols, et al., 2013; Smith, Symes, Lawson, & Morris, 1981; Tako & Nakamura, 1984, 1988), these studies focus mainly on the conformational aspects. Moreover, these studies only characterize chemically modified xanthan, and processing often includes heating and cooling steps, which are known to alter the conformation and therefore its physicochemical properties (Bradshaw, Nisbet, Kerr, & Sutherland, 1983; Khouryieh et al., 2007). Some studies exist, which describe xanthan-variants produced by genetic modification of *X. campestris* (*Xcc*), however, they only describe the impact of substitution-pattern on the

viscosity in dilute systems (Hassler & Doherty, 1990). While a recent study describes a genetically modified xanthan variant, the sole focus is on a maximum pyruvylated xanthan variant lacking acetylation of both mannose residues (Wu et al., 2018). The aim of this study is therefore to give an in-depth rheological characterization of xanthan-variants with defined acetylation and pyruvylation-patterns. These variants are produced by genetically modified *X. campestris* LMG 8031 strains, under mild conditions, to yield the most natural conformation of the modified polysaccharide variants. Another key aspect of this study is the investigation of the influence of cations on these variants. A comparison with most recent studies on xanthan's structure will give a revised insight on the structure-function-relationship of xanthan and elude how acetylation and pyruvylation influences its rheological properties in the absence and presence of salts. These variants are interesting for industrial application as they can be produced under identical established biotechnological production methods while having tailor-made properties like increased or decreased viscosity as well as altered impact of salt content or temperature on the rheological properties of the product. These properties can make the superior to the wild type concerning higher temperature stability or salt tolerance, as necessary for example in enhanced oil recovery or some cosmetic formulations.

2 Materials and methods

2.1 Fermentative cultivation of strains and production of xanthan

Xanthomonas campestris pv. campestris LMG 8031 (*Xcc*) (BCCM, Gent, Belgium) and deletion variants thereof were cultured at 30 °C in MM1 P100 as previously described (Rütering, Schmid, Rühmann, Schilling, & Sieber, 2016) containing 30 g L⁻¹ glucose as carbon source. The fermentative production of xanthan and engineered variants thereof were carried out in a 2 L-benchtop fermenter (Biostat B plus, Sartorius AG, Germany) equipped with two 6 blade-stirrers over 48 h with a controlled pH of 6.8 and a pO₂ of 30% saturation. All fermentations were performed with a starting OD of 0.1 by inoculation with an appropriate volume of preculture. The precultures were grown in 50 ml of MM1 P100 Media containing 30 g L⁻¹ glucose in 250 ml baffled Erlenmeyer-flasks over night at 250 rpm, 30 °C.

2.2 Preparation of competent Cells

Electrocompetent *Xanthomonas* cells were produced by a method described by Wang *et al* (2016), with minor variations (Wang, Zheng, & Liang, 2016). In detail, 50 ml of cell cultures were grown to an OD₆₀₀ between 0.6 and 1.0, centrifuged (7,500 g, 20 °C, 5 min) in a 50 ml conical tube, the pellet was washed in 20 ml 250 mM sucrose 3 times by resuspending and centrifugation (7,500 g, 20 °C, 5 min) and finally resuspended in 1 ml of 250 mM sucrose. 100 µl aliquots were used right away for transformation or stored at -80 °C.

2.3 Creation of *Xanthomonas* deletion-mutants

For the creation of deletion mutants, homologous recombination with pK19Gm, a derivative of pK19mobsacB with the kanamycin resistance exchanged with gentamicin resistance was applied. For the deletion of genes in *Xcc* two 500 base pair (bp)-fragments up- and downstream of the genes of interest were amplified via PCR, using isolated genomic DNA (gDNA) from *Xcc* as a template. Primers were designed based on the draft genome of *X. campestris* LMG 8031 (Schmid, Huptas, & Wenning, 2016). The amplified fragments were fused via overlap extension PCR, gel-purified and digested with restriction enzymes according to the introduced restriction sites. The plasmid was digested with the same restriction enzymes as the fused flanks and dephosphorylated by adding 0.25 µl of alkaline phosphatase to the restriction digest 15 minutes before terminating the reaction, in order to prevent re-ligation. The digested plasmid was purified by agarose gel-extraction. Vector and insert were ligated using T4-ligase. 10 µl of the reaction were used to transform *E. coli* DH5a. The correctness of the constructs was validated by colony-PCR and sequencing. *X. campestris* cells were transformed by electroporation, using 600-1,000 ng of pK19Gm plasmid carrying the respective fused flanks of the gene of interest. After electroporation, the cells were flushed with 1 ml of Super Optimal Broth with catabolite repression (SOC) media (20 g L⁻¹ tryptone, 5 g L⁻¹ yeast extract, 0.5 g L⁻¹ NaCl, 10 mM MgSO₄, 10 mM MgCl₂, 2.5 mM KCl, 20 mM glucose) and agitated at 250 rpm for 2-3 h at 30 °C. After plating the cells on LB-Agar containing 30 µg ml⁻¹ gentamicin, a single colony was subsequently cultivated in LB media without antibiotics for 24 h. The second homologous recombination event was triggered by plating dilution series onto LB-Agar containing 10 % (w/v) sucrose. Gene deletions were verified by colony-PCR.

2.4 Recovery of xanthan-variants

For the recovery of the different xanthan-variants, the fermentation broth was diluted 1:10 and centrifuged (15,000 g, 20 min, 20 °C) to separate the cells from the xanthan containing aqueous phase. The supernatant was subsequently concentrated back to the initial volume by crossflow filtration using an ultrafiltration cassette (Hydrosart®, Sartorius AG, Germany) with a molecular weight cutoff of 100 kilodaltons (kDa). The concentrated supernatant was poured into 2 volumes of 2-propanol under stirring conditions (170 rpm). The precipitated xanthan was dried in a vacuum oven at 45 °C for 48 h and after the gravimetric determination of the dry mass, it was milled into a fine powder in a ball mill (Mixer Mill MM 400, RETSCH GmbH, Germany) at 30 Hz for 30 s.

2.5 Rheology

2.5.1 Sample preparation

For the determination of rheological properties 1 % (w/w) solutions of the xanthan-variants were prepared in a total amount of 200 g ddH₂O. The samples were prepared in a 1 l Erlenmeyer flask by shaking over night at 250 rpm at 50 °C. 50 g of the salt-free solution was used directly for all measurements. 49 g and 48 g of the sample were mixed with 1 ml of a 25 % (4.28 M) NaCl-solution and 2 ml of a 23.5 % (2.12 M) CaCl₂-solution, respectively, to obtain a total concentration of 85 mM for each approach. All samples were centrifuged (500 g, 2 min, 20 °C) in order to remove any air bubbles, which might occur during mixing and stored at 4 °C over night prior to measurements.

2.5.2 Rheological measurements

Rheological measurements were carried out with a stress-controlled MCR300 rotational rheometer (Anton Paar GmbH, Austria) equipped with a CP 50-1 cone-and-plate measuring system, 50 mm diameter, 1° cone angle and 50 µm cone truncation (Anton Paar GmbH, Austria) and a Peltier controlled TEK 150P temperature unit (Anton Paar GmbH, Austria). All measurements, except the temperature sweeps, were carried out at 20 °C and all samples were incubated in the measuring system at 20 °C for 5 minutes prior to the measurement. All experiments were carried out in triplicates.

2.5.3 Flow curves

Determination of flow curves were carried out at a logarithmically increasing shear rate from 10^{-3} - 10^3 s^{-1} by measuring 4 data points per decade with a decreasing measuring time of 100 - 5 s per data point.

2.5.4 Amplitude sweeps

Amplitude sweeps were performed at a logarithmically increasing shear stress amplitude from 10^{-1} - 10^2 Pa with a frequency of 1 Hz.

2.5.5 Frequency sweeps

Frequency sweeps were carried out in the linear viscoelastic region (LVE) at a logarithmically increasing frequency from 10^{-2} – 10^1 Hz.

2.5.6 Temperature sweeps

Temperature sweeps were performed within the LVE at a frequency of 1 Hz. A discrete temperature-ramp from 20 to 75 °C at a heating rate of 4 °C min^{-1} was applied. To prevent evaporation, the edge of the sample was covered with low viscosity paraffin oil (Carl Roth GmbH & Co. KG, Karlsruhe, Germany).

2.5.7 Thixotropy

Thixotropic behavior of the samples (salt free, 85 mM NaCl, 85 mM $CaCl_2$) was evaluated by a 3-stage oscillatory shear. During the first stage the sample was measured within the previously determined LVE-region followed by a high oscillatory shear of 10^2 Pa. The recovery of the structure was then measured over 10 min within the LVE region.

2.6 Analytical methods

2.6.1 Determination of monomer composition

Determination of the monomer composition was performed by the 1-phenyl-3-methyl-5-pyrazolone-high throughput method (HT-PMP) (Rühmann, Schmid, & Sieber, 2014). For this a 0.1 % xanthan-solution was prepared by dissolving the powder in ultrapure water under stirring (250 rpm, room temperature). Samples were subsequently hydrolyzed by adding 20 μ l of 4 M trifluoroacetic acid (TFA) to 20 μ l in a 96-well PCR plate, sealing with a rubber lid and sealing the plate in a custom made metal device. Hydrolysis was carried out at 121 °C over 90

min in a sand bath. After hydrolysis the samples were neutralized by the addition of 3.2 % NH_4OH . The required volume was previously determined using 2 M TFA and phenol red as indicator. Derivatization was done by the addition of 75 μl PMP-mastermix to 25 μl of neutralized hydrolysate and incubation at 70 °C for 100 min in a thermal cycler. After derivatization 20 μl of the sample were mixed with 130 μl of 26-fold diluted 0.5 M acetic acid, mixed using the metal device and subsequently filtered through a 0.2 μm Filter plate (1000 g, 5 min, 20 °C). The 96-well microtiter plate was subsequently sealed with a silicone capmat and placed in the autosampler for HPLC-MS/MS measurements.

2.6.2 Determination of acetate and pyruvate content

For the determination of the acetyl- and pyruvyl-groups, 10 ml of 1 % solution of the different xanthan-variants were prepared under the same conditions as described in 2.5.1, and hydrolyzed in 250 mM sulfuric acid for 5 h at 90 °C. After cooling the samples were centrifuged (21,000 g, 1 min) and filtered through a 0.22 μm PVDF syringe filter (Restek GmbH, Bad Homburg, Germany). The Samples were subsequently analyzed via HPLC on a Rezex ROA H^+ -column (Phenomenex Inc, Torrance CA, USA) without further processing. For calibration a 5 mM pyruvate and 16.7 mM acetic acid standard was used.

2.6.3 Molecular weight determination

0.1 % (w/v) of untreated EPS-powder was dissolved in 0.1 M LiNO_3 at 50 °C for 12 h under stirring (250 rpm). Treated samples (0.5 % (w/v), 85 mM NaCl, pH 5.5) were diluted to a concentration of 0.1 % (w/v) and no further treatment was applied prior to measurements. Determination of molecular weight was carried out via size-exclusion chromatography (SECcurity GPC System, PSS Polymer Standards Service GmbH, Germany) with a SECcurity GPC1260 RI-Detector and a SECcurity SLD7000 7-angle light-scattering detector. Separation was performed by a Suprema 100 Å column coupled with two Suprema 10,000 Å columns and a Suprema guard column at 50 °C using 0.1 M LiNO_3 as eluent at a flow rate of 1 ml/min. 100 μl of sample was used for analysis.





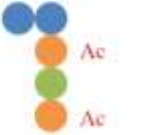



3 Results and Discussion

3.1 Creation of deletion variants

The knockout of the two acetyltransferases GumF and GumG was performed in one step using the upstream flank of *gumF* and the downstream flank of *gumG*, as these genes are directly adjacent to each other in the *gum*-cluster, creating the mutant *Xcc* Δ *gumFG*. The fused flanking regions were cloned into the pK19Gm plasmid and transferred to *X. campestris*. Using the up- and downstream flanks of the pyruvyltransferase *gumL*, *Xcc* Δ *gumL* was created. The variant Δ *gumFGL* was designed by knocking out *gumL* in *Xcc* Δ *gumFG*. All knockouts have been verified via sequencing of the knock-out region on the chromosome. All knockout-variants did not grow on Gentamicin, indicating the markerless deletion of the genes. Additionally, the single knockout of the acetyltransferase *gumG* was achieved by using the same downstream flank as for creation of *Xcc* Δ *gumFG* and the upstream flanking region of *gumG*. As the double deletion mutant *Xcc* Δ *gumGL* was not successful, this variant was obtained by a plasmid-based re-establishment of the GumF acetyltransferases in the Δ *gumFGL* deletion mutant, using the IPTG-inducible pSRKGm broad host expression vector, harboring the *gumF* gene. Sequencing results of the deletion variants are given in Figure S1.

3.2 EPS Production and analysis

All xanthan-variants were produced in a 1.5 L-bioreactor scale within 48 h. As the strains *Xcc* *wt*, *Xcc* Δ *gumFG*, *Xcc* Δ *gumFGL*, *Xcc* Δ *gumL* and *Xcc* Δ *gumG* were markerless knock-out variants, they were cultivated without antibiotics. Since the strain *Xcc* Δ *gumGL* harbored the pSRKGm-plasmid with *gumF*, the strain was cultivated using 30 mg ml⁻¹ Gentamicin. The total product yields in dry mass of EPS before milling are given in Figure 1.

Strain	<i>Xcc wt</i>	<i>Xcc AgumF</i>	<i>Xcc AgumG</i>	<i>Xcc AgumFG</i>
Variant	Xanthan	Xan Δ F	Xan Δ G	Xan Δ FG
Repeating unit				
Yield [g/l]	18.03	11.30	10.91	16.87
Productivity [g l ⁻¹ h ⁻¹]	0.27	0.24*	0.15	0.23
Strain	<i>Xcc AgumL</i>	<i>Xcc AgumFL</i>	<i>Xcc AgumGL</i>	<i>Xcc AgumFGL</i>
Variant	Xan Δ L	Xan Δ FL	Xan Δ GL	Xan Δ FGL
Repeating unit				
Yield [g/l]	15.95	11.34	11.10	17.35
Productivity [g l ⁻¹ h ⁻¹]	0.24	0.45**	0.15	0.26

* Total reaction volume: 1 l

● Glc ● Man ● GlcA ● Ac Acetate ● Pyr Pyruvate

** Fermentation cancelled after 25 h

Figure 1 Schematic representation of the acetylation and pyruvylation-patterns of the produced xanthan-variants. Production yields and productivity of the strain are given below each variant.

For the analysis of the monomer-composition, a 0.1 % solution of the dried powder of each cross-flow purified xanthan variant was hydrolyzed. Before hydrolyzation a part of the solution was used for the enzymatic detection of residual glucose or pyruvate in the xanthan solution. No significant amounts of glucose or pyruvate could be detected in the supernatant. After hydrolyzation a part of the neutralized solution was used to determine the pyruvate content of each xanthan variant. The calculated recovery ranged from 32.55 % to 40 %. All xanthan-variants had similar Glc:Man:GlcA ratios (Figure S3) and the molecular weight of the variants were within the same order of magnitude (Table 1), indicating that the deletions of the pyruvyl- and acetyl-transferases had no effect on monomer composition or polymer chain length.

Table 1 Calculated M_w of xanthan variants. M_w was obtained by GPC-analysis of 0.1 % xanthan in 0.1 M LiNO_3 using pullulan standards of different M_w (348 Da-2.35 MDa) for calibration.

Variant	M_w [Da]
Xan	$2,3 * 10^7$
Xan Δ F	$4,5 * 10^7$
Xan Δ G	$2,2 * 10^7$
Xan Δ FG	$2,5 * 10^7$
Xan Δ L	$1,8 * 10^7$
Xan Δ FL	$2,2 * 10^7$
Xan Δ GL	$1,6 * 10^7$
Xan Δ FGL	$1,8 * 10^7$

3.3 Effect of deletions of acyltransferases on acetylation and pyruvylation patterns

Acetate and pyruvate contents were determined by hydrolyzing a 1 % solution of each xanthan variant and subsequent analysis of the supernatant of the hydrolysate via HPLC-UV. An overview of acetate and pyruvate content is given in Figure 2.

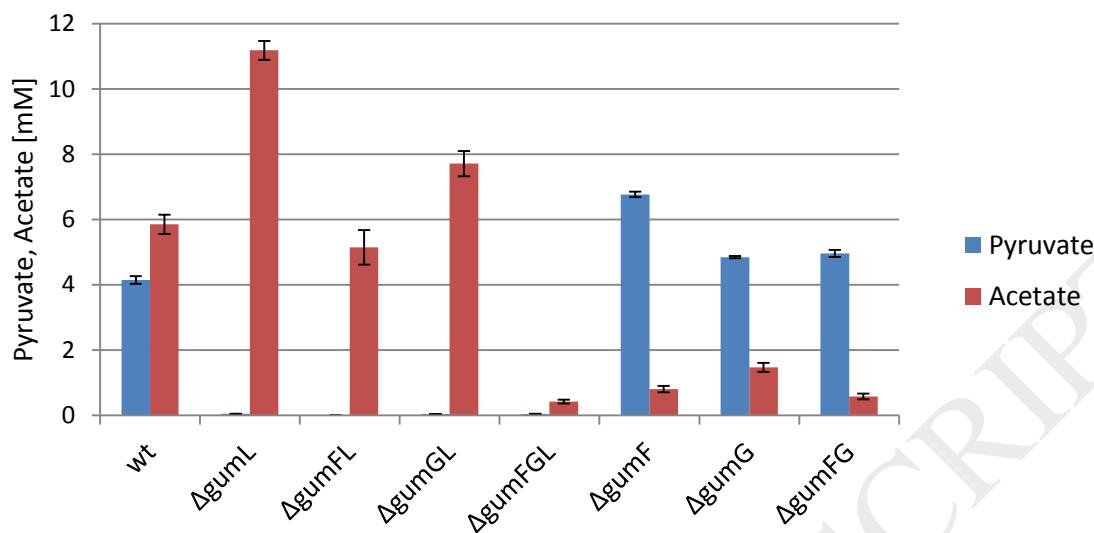


Figure 2 Acetate and pyruvate content of the different xanthan-variants after hydrolysis with 0.25 M H₂SO₄. All samples were dissolved in ddH₂O at a concentration of 10 g l⁻¹ and 72 % H₂SO₄ was added to a final concentration of 0.25 M. All samples were hydrolyzed in triplicates. The error bars show the standard deviation of triplicates.

Xanthan produced by the wildtype strain (wt) showed an acetate to pyruvate ratio of 1.5:1 and a calculated acetate and pyruvate amount of 2.5 % and 3.5 % respectively. However, due to the calculated recovery of 62.5 % by the HT-PMP method (Figure S3) acetate and pyruvate content accord to 4.0 % and 5.6 % respectively, which is well in the range of previously reported values (Candia & Deckwer, 1999; Kennedy & Bradshaw, 1984; Tako & Nakamura, 1988). The depyruvylated variants (XanΔL, XanΔFGL, XanΔFL and XanΔGL) showed no quantifiable amounts of pyruvate after hydrolysis, indicating the complete depyruvylation of the polysaccharide. The amount of acetate in these variants varied depending on the knockout of the acetyltransferases GumF and GumG. With both functional acetyltransferases present, the acetate content of XanΔL almost doubled compared to xanthan from the wildtype, indicating a competition of pyruvate and acetate in respect to the outer mannose. We hypothesize that without the competing pyruvate, the available positions for acetylation by GumG increases and therefore, the overall acetate content rises. XanΔFL, lacking the acetyltransferase for the inner mannose showed considerably lower amounts of acetate compared to XanΔL, which were comparable to the unmodified xanthan. In contrast, XanΔGL lacking the outer acetate and pyruvate showed higher amounts of acetate compared to both XanΔFL and xanthan from the wildtype, indicating, that the inner mannose is more frequently acetylated than the outer mannose, when no pyruvate is present at the outer mannose. Previous studies report acetylation

of 60-70% of the inner mannose, which is in good accordance with our findings in this variant (Abbaszadeh et al., 2015). Xan Δ FGL had no quantifiable amounts of pyruvate and the acetate content decreased 14-fold compared to the natural xanthan and lays within the detection limit of the analysis. Unexpectedly, the degree of pyruvylation was highest in Xan Δ F, which lacks acetylation of the inner mannose, rather than in Xan Δ G. This opposed our expectations, as the latter lacks acetylation of the outer mannose, which would result in more free positions for pyruvylation. Both Xan Δ G and Xan Δ FG showed very similar degrees of pyruvylation, which were comparable to native xanthan. Xan Δ F, Xan Δ G and Xan Δ FG exhibited a drastic decrease of acetylation compared to all other variants with a pyruvylation of the outer mannose. The higher pyruvate content of Xan Δ F compared to Xan Δ G can be explained by the competition for acetylation and pyruvylation of the outer mannose. While only the outer mannose can be acetylated in Xan Δ F, and the pyruvylation of outer mannose additionally reduces the positions for acetylation, this would explain the lower amount of acetate in this variant. On the other hand, the permanently available spot for acetylation of the inner mannose by GumF in Xan Δ G could explain the higher amounts of acetate of Xan Δ G. Overall acetate content of Xan Δ FL and Xan Δ GL indicates that without pyruvylation the inner mannose seems to be more frequently acetylated than the outer mannose, proved by the higher amount of acetate in Xan Δ GL compared to Xan Δ FL, which confirms previous reports of high degrees of acetylation of the inner mannose (Abbaszadeh et al., 2015; Hassler & Doherty, 1990). The acetate-concentrations in Xan Δ FL were also quite comparable to those reported by Hassler et al (1990)., who also report no pyruvate and a slightly decreased degree of acetylation compared to unmodified xanthan (Hassler & Doherty, 1990). On the other hand, acetate content of Xan Δ G, which is pyruvylation on the outer mannose, indicates a rare acetylation of the inner mannose in the presence of pyruvate on the outer mannose. This is interesting, as this variant should theoretically have the same amount of acetate as Xan Δ GL. However, pyruvylation of the outer mannose seems to impact the acetylation of the inner mannose drastically. These findings contradict the data reported by Hassler et al (1990)., who reported a degree of acetylation of this variant similar to unmodified xanthan (Hassler & Doherty, 1990). As the degree of acetylation of Xan Δ F is as low as in Xan Δ FG, this gives further evidence for competition of acetylation and pyruvylation of the outer mannose and that the inner mannose is more often acetylated than the outer mannose.

3.4 Rheological characterization of the xanthan-variants

As the rheological properties of xanthan are quite dependent of ionic strength (Dário et al., 2011; Rochefort & Middleman, 1987), the scope of this work was to characterize the influence of defined acetylation and pyruvylation patterns of xanthan on its rheological properties including evaluation of the effect of cations on the variants. For rheological characterization, natural xanthan (Xan) as well as the seven different xanthan-variants (Xan Δ F, Xan Δ G, Xan Δ L; Xan Δ FG, Xan Δ FGL, Xan Δ FL, Xan Δ GL) produced by genetically modified *X. campestris*-strains, resulting in distinct acetylation and pyruvylation patterns have been thoroughly characterized in salt free solution as well as in presence of mono- and divalent cations, by the addition of NaCl and CaCl₂, respectively. For comparison a 1 % solution of each xanthan variant and salt concentrations of 85 mM have been chosen, as these concentrations resulted in differences in rheological characteristics, which were optimal for describing the effects of modifications of the polysaccharide. For better comparability, the conductivities of all salt-free solutions and the ones of the solutions containing 85 mM NaCl or CaCl₂ were measured and are summarized in Table S2.

3.4.1 Effect of acetylation and pyruvylation patterns on viscosity

It has been widely accepted that depyruvylation of xanthan leads to a decrease of its viscosity (Callet et al., 1987; Cheetham & Norma, 1989; Erten, Adams, Foster, & Harding, 2014; Tako & Nakamura, 1988). Common theory is that pyruvate destabilizes the ordered structure of xanthan and by depyruvylation a more ordered structure is obtained (Sandford, Pittsley, Knutson, Watson, & Cadmus, 1977; Shatwell, Sutherland, Dea, & Ross-Murphy, 1990). Correlation with viscosity this in turn means, that the ordered structure of xanthan is responsible for a lower viscosity, especially at lower shear rates, as high viscosity at low shear rates can be explained by interactions of random coils of the exopolysaccharide, especially at high concentrations. This could be easily confirmed by our studies with the variant Xan Δ L, which showed a decreased viscosity by two orders of magnitude compared to unmodified xanthan (Figure 3). The distinct η_0 , which was absent in the xanthan produced by the wildtype further demonstrates the drastically decreased viscosity by depyruvylation. Furthermore, this variant showed increased degree of acetylation, which can be contributed to an increase of available position for acetylation of the outer mannose, as it cannot be pyruvylated anymore. The effects of different acetylation patterns and their combination with depyruvylation on the

other hand were quite variable and to some extent puzzling. As described before, the degrees of acetylation in all variants lacking pyruvylation could be correlated with a higher degree of acetylation on the inner mannose as well as an increase of acetylation of the outer mannose in absence of the pyruvate-ketal. The degrees of acetylation and also pyruvylation of the xanthan-variants still having the pyruvate-ketal were against our expectations quite contradictory and so was their effect on the rheological properties. As the acetyl-groups in the sidechain are reported to stabilize the ordered structure of xanthan (Shatwell et al., 1990), a higher degree of acetylation would result in a decrease of viscosity and vice versa. Previous studies showed that while deacetylation leads to decreased viscosity in dilute concentrations, this effect is reversed at higher concentrations, which confirms the stabilizing effect of the acetate groups (Khouryieh et al., 2007; Tako & Nakamura, 1984). However, most of the investigated variants were produced chemically, and therefore no reliable information of the acetylation-pattern could be concluded. One of the few rheological analyses of xanthan modified by genome editing of *X. campestris* by Hassler & Doherty (Hassler & Doherty, 1990) was carried out with xanthan concentrations below 0.2 % and therefore the reported effects of acetylation are in the range of dilute solutions. The low viscosity of Xan Δ L compared to unmodified xanthan could therefore be both correlated with the absence of the pyruvate-ketal in combination with the higher degree of acetylation, which would further stabilize its ordered structure. As shown by the acetylation patterns of Xan, Xan Δ F and Xan Δ G the inner mannose is already highly acetylated. The high amount of acetate of Xan Δ L can therefore be explained by a higher degree of acetylation of the outer mannose due to absence of the pyruvate-ketal. Interestingly the deacetylated variants Xan Δ F and Xan Δ FG showed almost unaltered viscosity to unmodified xanthan. As both variants showed very low degrees of acetylation, which can be attributed to the missing acetylation of the inner mannose and a competing acetylation and pyruvylation of the outer mannose in Xan Δ F or a complete lack of acetylation in Xan Δ FG, there seems to be little effect of acetate on the viscosity of xanthan. As Xan Δ F shows higher degree of pyruvylation and by the ways of creating this variant, the deacetylation would only affect the inner mannose. As we suggest there is a competition for acetylation and pyruvylation, we predict a similar acetylation pattern in Xan Δ FG, however with an overall lower degree of pyruvylation. As these variants show very similar flow behavior compared to unmodified xanthan, this would contribute very little influence of deacetylation of xanthan on its rheological properties when the polysaccharide is pyruvylation. While Xan Δ G has an identical

degree of pyruvylation as Xan Δ FG and only a very small, however considerably higher amount of acetylation compared to Xan Δ F and Xan Δ FG, it is the only deacetylated variant carrying the pyruvate ketal at the outer mannose. From the nature of creating the variant we predict that this small amount of acetate is bound to the inner mannose, contributing a highly stabilizing effect to the acetate group bound to the inner mannose. This becomes further evident by comparing Xan Δ FL, Xan Δ FGL and Xan Δ GL to Xan Δ L. While all four variants lack pyruvylation of the outer mannose, only Xan Δ GL and Xan Δ L are acetylated on the inner mannose, which results in a drastically reduced viscosity. The relative high amount of acetylation of the outer mannose in Xan Δ FL on the other hand has no further impact on the viscosity, which stays unaltered compared to Xan Δ F. This would mean that acetylation of the outer mannose in the absence of pyruvate and acetate on the inner mannose has a significantly smaller stabilizing effect compared to acetylation of the inner mannose compared in absence of the pyruvate ketal. The high viscosity of Xan Δ FGL compared to Xan Δ L can be explained by the lack of stabilizing acetyl-groups, somehow cancelling out the stabilizing effect of depyruvylation. While all xanthan-variants still containing the pyruvate-ketal showed increased viscosity after the addition of cations, the species (mono- or divalent cations) had no impact on the increase of viscosity. All variants lacking the pyruvate-ketal showed a decrease of viscosity in the presence of cations, while the effect of Ca²⁺-ions was slightly bigger compared to monovalent Na⁺-ions. These results are consistent with previous studies, which report the involvement of the pyruvyl-groups and the termini of the main chains in the interactions with cations (Bergmann et al., 2008). The influence of cations was generally higher at low shear rates, with diminishing effects towards higher shear rates. One exception was Xan Δ F, where the viscosity curves were higher throughout the investigated shear rates, resulting in a parallel trend of flow behavior in the presence and absence of cations. The diminishing effect of cations can be explained by high shear forces breaking up intermolecular cation mediated interactions, which are stable under low-shear conditions. The absence of this effect in Xan Δ F could be due the higher degree of pyruvylation, leading to increased intermolecular forces, which are more stable under high shear rates. While the addition of cations had a reduced effect on the viscosity of Xan Δ FG it showed almost no effect on the viscosity of Xan Δ G. As both of these variants show similar pyruvate levels, but Xan Δ G is still acetylated on the outer mannose, this raises the question if and how the ordered and unordered structure influence the intermolecular interactions mediated by cations. However, there might

also be a synergistic effect between the decrease of viscosity by a higher degree of ordered structure and the interactions of cations. As all depyruvylated xanthan-variants showed decreased viscosity in the presence of cations, and in the case of Xan Δ FGL, where we assume a higher degree of unordered structure due to the lack of acetyl-groups this effect may only be attributed to the absence of pyruvyl-groups and does not correlate with the ordered or unordered structure.

ACCEPTED MANUSCRIPT

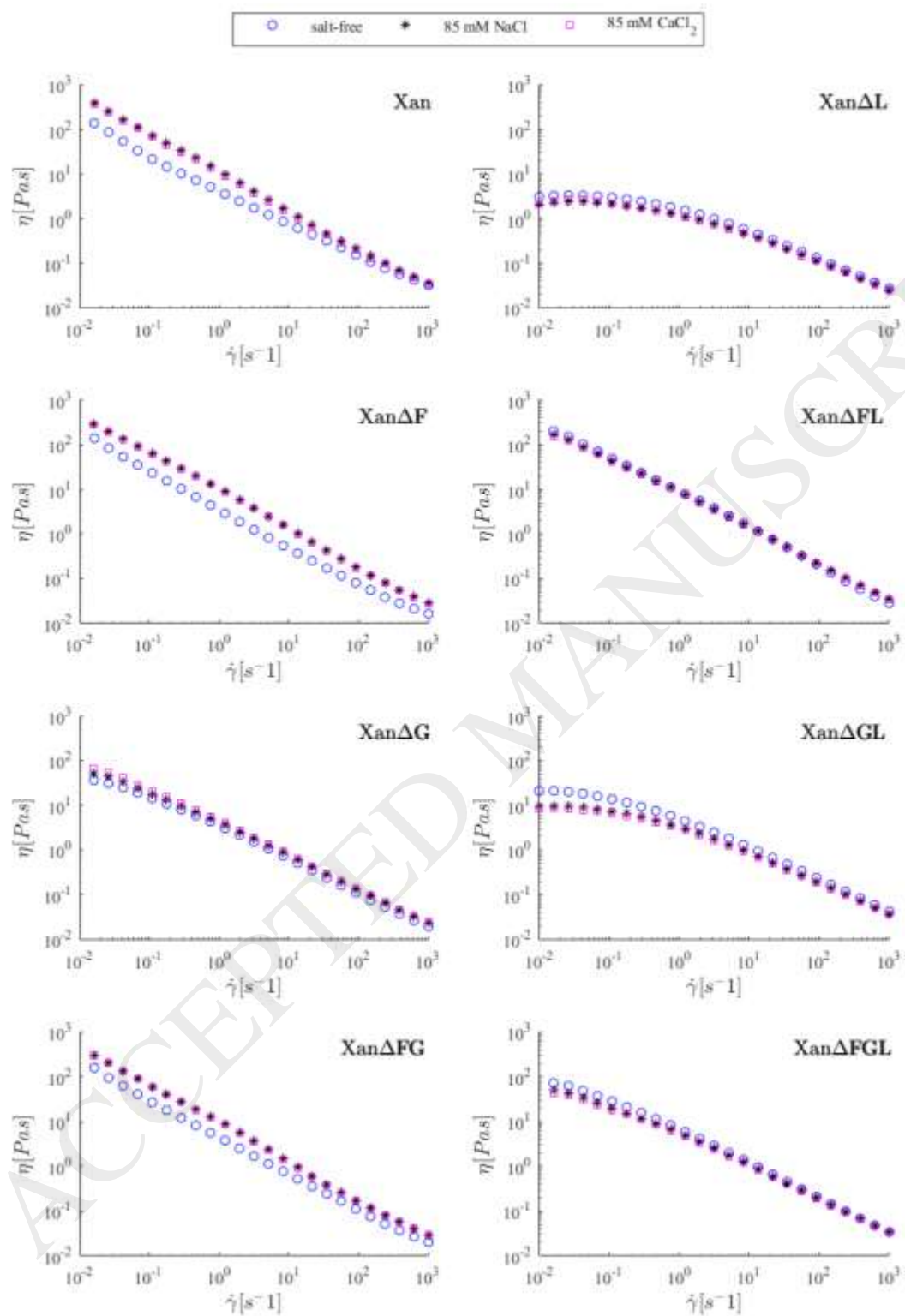


Figure 3 Flow curves of 1 % solutions of xanthan-variants, salt-free (o), 85 mM NaCl (*), 85 mM CaCl₂ (□) measurements were carried out in triplicates, from a shear rate from 10⁻² to 10³ s⁻¹ at 20 °C. All samples rested for 5 min after application on the rheometer before measuring, to avoid shear-induced starting conditions.

3.4.2 Effect of acetylation and pyruvylation patterns on oscillatory shear behavior

While the flow curves already gave good and detailed impression about the properties of the different xanthan-variants, they inherit the problem giving information of a sample whose structure is irreversibly destroyed. In order to get more detailed information about the rheological properties, all variants were tested under oscillatory shear within the linear-viscoelastic (LVE) region. In order to determine the LVE for each sample an amplitude sweep was carried out (Figure S4). Additionally, it was tested, if any structural destruction was reversible by performing a thixotropy test for each variant. Amplitude sweeps revealed, that at the chosen frequency of 1 Hz all xanthan-variants had gel character with $G' > G''$ to a certain extent within the LVE. One exception was Xan Δ L, which showed liquid behavior ($G' < G''$). Unmodified xanthan showed gel strength of 14.4 Pa and a damping factor of 0.42. Upon the addition of cations, gel strength increased drastically from 14.4 Pa to 26.7 and 29.5 Pa for CaCl₂ and NaCl, respectively, while $\tan\delta$ decreased towards 0.25 and 0.24 respectively, resulting in an overall stronger, elastic gel. Upon addition of cations, the gel structure also became more brittle as indicated by an increase of G'' at the end of the LVE region. However, the LVE also increased towards higher deformation values and the gel-sol transition shifted considerably towards a higher strain. Variants Xan Δ F and Xan Δ FG showed similar behavior, however the addition of cations had less influence on the gel strength Xan Δ F and even less on Xan Δ FG. The lowest effect of cations was observed in Xan Δ G, which had overall weaker gel strength, and even with the addition of salts no increase of G'' was observed, indicating a very weak gel structure. As observed in rotational shear experiments, the addition of salts had a contrary effect on the gel strength on all depyruvylated variants. As already mention Xan Δ L showed no gel character but liquid character. Depyruvylation in combination with deacetylation of the outer mannose (Xan Δ GL) lead to an increase in overall gel strength, however G'' also increased, leading to an overall increase $\tan\delta$ and therefore a very weak gel structure. The same effect was observed for Xan Δ FL and Xan Δ FGL, however not as prominent as in Xan Δ G and comparing all three variants this effect was least prominent in Xan Δ FL.

Frequency sweeps further supported our findings and showed a typical gel behavior for Xan, Xan Δ F and Xan Δ FG with a low frequency dependency of both G' and G'' . Across the investigated frequency range from 0.01 to 10 Hz no crossover of G' and G'' , was observed, indicating relaxation times >100 s and an elastic gel structure, which would remain stable

during long term storage of the samples (Figure 4). For these three variants addition of cations resulted in a higher overall gel strength and the frequency dependency of G' and G'' further decreased compared to the solutions without cations. Xan Δ G as the only deacetylated variant which still contains the pyruvate ketal on the other hand showed a relatively low relaxation time between 25 and 40 s (given by the inverse of a G' and G'' crossover frequency between 0.025 Hz and 0.04 Hz) indicating a gel character with low elastic portion and a loss of a stable long term gel-character. The depyruvylated variants Xan Δ L, Xan Δ FL, Xan Δ GL and Xan Δ FGL all showed relatively short relaxation times between 0.1 and 100 s. Xan Δ L shows the lowest one of 0.1 s and no gel character across a wide frequency region, demonstrating that depyruvylation leads to a complete loss of gel character in xanthan. The weak gel character at higher frequencies could be attributed to entanglements of the molecules, however it is still very weak and investigations at higher frequencies would be needed to confirm whether the weak gel character is stable at high frequencies. While Xan Δ FGL showed a relaxation time between 25 and 40 s, Xan Δ FL only indicated a transition point at frequencies below 0.01 Hz, resulting in a relaxation time >100 s. The relatively low relaxation times of the depyruvylated xanthan variants confirm weak gel structures, which are attributed to the depyruvylation, resulting in a more ordered helical structure of the xanthan chains and thereby reducing the gel strength, which we propose to be due to random-coil entanglements, especially at low frequencies. This theory is further supported by the findings for Xan Δ L, which showed liquid character over a wide frequency with a relaxation time of 0.1 s, meaning than Xan Δ L showed weak gel properties at high frequencies. This is a typical behavior of a Maxwell fluid. The sol character of Xan Δ L over a wide frequency further backs the hypothesis of a highly ordered structure caused by depyruvylation combined with the increase of acetylation. At low frequencies these helical rods could flow easily past each other, while at high frequencies more entanglements would occur resulting in a slight gel character. Interestingly Xan Δ GL exhibited characteristics very similar to Xan Δ L. Comparing the acetate content of Xan Δ GL with Xan Δ L (Figure 2), as Xan Δ GL has the second highest degree of acetylation after Xan Δ L we conclude that the high acetate content is due to acetylation of the inner mannose. From the rheological data we conclude, that the inner acetate is primarily responsible for the stabilization of the helical structure, leading to a decrease in viscosity and gel-strength. While Xan Δ F shows a degree of acetylation comparable to the native xanthan but exhibiting a sol-gel transition at low frequencies, we conclude, that acetylation of the outer mannose also affects the stability

of the helical structure, but to a far less extent compared to acetylation of the inner mannose. Xan Δ FGL, which is completely deacetylated and depyruvylated still exhibits gel characteristics over a wide frequency range, which is slightly lower than Xan Δ FL. From a structural point of view and considering our previous conclusion that the ordered structure is responsible for higher viscosity and gel-strength, this would mean that the structure of xanthan is a more ordered one without any decoration compared to Xan Δ FL and Xan Δ GL, where the outer or inner mannose is still acetylated. From this data we can propose certain effects on how complete deacetylation and depyruvylation affects the structure of xanthan, however more information about its structure is necessary for a defined statement.

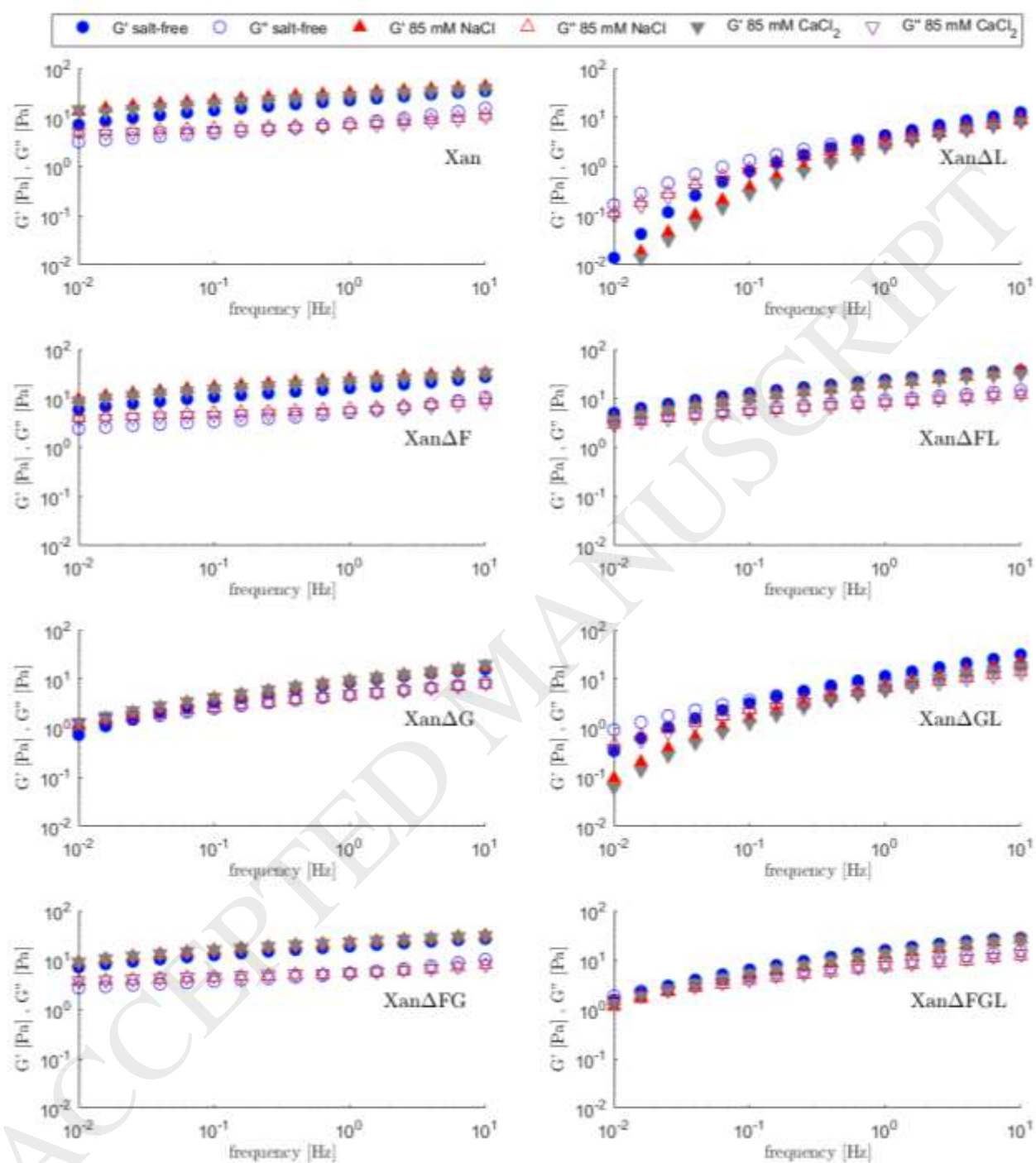


Figure 4 Frequency sweeps of salt free 1 % xanthan solutions and with 85 mM NaCl or 85 mM CaCl₂. Storage moduli G' (filled symbols) and loss moduli G'' (empty symbols) are shown without salt (\bullet/\circ), with 85 mM NaCl (\blacksquare/\square) and 85 mM CaCl₂ (\blacktriangle/\triangle). All measurements were performed under a constant shear stress of 1 Pa and logarithmically increasing frequency amplitude from 0.01 to 10 Hz.

3.4.3 Effect of acetylation and pyruvylation patterns on temperature dependency of rheological properties

Next to mechanical stress, temperature plays an important role for the rheological properties of xanthan by its transition of the ordered-disordered structure (Matsuda, Biyajima, & Sato, 2009; Milas & Rinaudo, 1979). To investigate the effect of acetylation and pyruvylation patterns on the temperature induced effects, oscillatory shear in the LVE-region was carried out by heating the samples from 20-75 °C with subsequent cooling to 20 °C (Figure 5). Table 2 gives an overview of all variants sorted by their temperature stability in the absence of cations based on the relative value of G' at 20 °C and 75 °C, as well as the influence of cations on the temperature stability. All variants showed a temperature dependency of their gel strength to different extents, while all effects were completely reversible. Unmodified xanthan showed high temperature stability and the addition of salts only lead to very slight increase of thermal stability. This may however be correlated to the increase of the gel strength upon addition of cations. The different deacetylation patterns lead to an evident decrease of gel strength upon heating. The effect was least evident in Xan Δ F, followed by the completely deacetylated Xan Δ FL and most pronounced in Xan Δ G. This behavior could be attributed to the reduced gel strength of Xan Δ G by higher acetylation of the inner mannose. For all deacetylated variants addition of salts lead to a much higher stabilization compared to mechanical stress. As stated before, the $-\text{COO}^-$ residues of pyruvylated xanthan seem to play a major role in the interactions of cations and the polymer and these interactions seem to have higher temperature stability than mechanical stability. Addition of salts to the depyruvylated variants had, as described before an adverse effect on the gel strength of xanthan, however compared to the salt-free systems, cations seem to somehow stabilize the structure during heating and cooling. This is especially evident by the missing sol-gel transition of Xan Δ FL/NaCl. A unique effect was observed for Xan Δ FL and Xan Δ FGL, by the distinct increase of both G' and G'' upon heating, which then again decreased upon further heating, resulting in a peak of the moduli at a certain temperature. As the state changes from sol to gel and to sol again, this indicates a temperature transition of the secondary structure of xanthan. As this phenomenon only occurred in variants lacking acetylation of the inner mannose, the acetylation at this position also seems to play a major role in the temperature induced structural changes of xanthan. Interestingly this effect did not occur upon cooling and it was also absent after the addition of salts. As this “peak” was most evident in Xan Δ FGL which had no acetate at all but far less distinct in Xan Δ FL, which has a

considerable degree of acetylation on the outer mannose, this effect could be due to masking effects of the outer acetate on the $-\text{COO}^-$ residue of the glucuronic acid. This could also explain why this effect is completely abrogated by the addition of cations. While under oscillatory measurements with varying mechanical stress, the addition of cations to the depyruvylated variants showed only minor effects, it becomes evident that they play a stabilizing role in structural transition of xanthan under thermal treatment, especially in the absence of acetate.

Table 2 Influence of temperature on the oscillatory shear behavior of the xanthan variants determined by the relative G' value at 20 °C and 75 °C. +/-: positive/negative effect of cations on temperature stability

Variant	G' 20°C [Pa] (salt free/with salt)	G' 75°C [Pa] (salt free/with salt)	Rel. gel strength at 75 °C [%]	Effect of salt on stability
Xan	24.7 / 28.1	15.7 / 16.1	63.6 / 57.4	-
Xan Δ F	17.1 / 22.8	6.1 / 14.5	35.7 / 63.6	+
Xan Δ FG	17.4 / 20.9	4.6 / 13.5	26.4 / 64.6	+
Xan Δ FGL	14 / 11.8	2.5 / 1.4	17.9 / 11.9	-
Xan Δ FL	19.9 / 19.3	3.5 / 4.5	17.6 / 23.3	+
Xan Δ GL	10.3 / 6.7	1.2 / 0.4	11.7 / 6.0	-
Xan Δ L	3.1 / 2.3	0.2 / 0.1	6.5 / 4.3	-
Xan Δ G	7.3 / 8.3	0.1 / 1.5	1.4 / 18.1	+

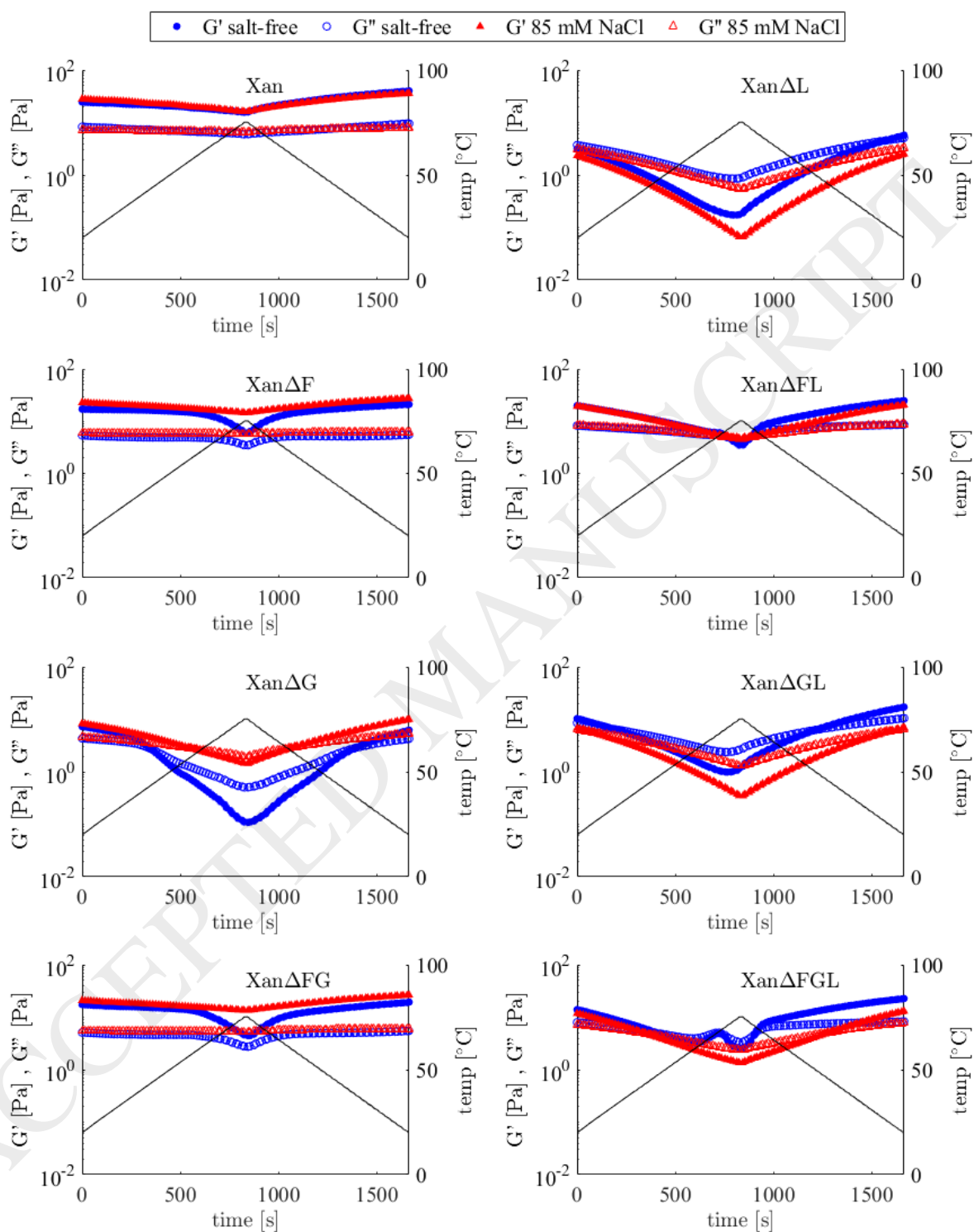


Figure 5 Temperature sweeps of 1 % xanthan solutions salt free and with 85 mM NaCl. Storage moduli G' (filled symbols) and loss moduli G'' (empty symbols) are shown without salt (\bullet/\circ), with 85 mM NaCl (\blacktriangle/\triangle). For better visibility, xanthan with CaCl_2 is not shown. Temperature sweeps were carried out with a discrete temperature ramp at a heating rate of $4\text{ }^\circ\text{C}$ per minute within the LVE at a shear stress of 1 Pa and a frequency of 1 Hz.

4 Conclusion

The seven different xanthan-variants with unique, highly specific acetylation and pyruvylation patterns (Xan Δ F, Xan Δ G, Xan Δ FG, Xan Δ FL, Xan Δ GL and Xan Δ FGL) showed distinct rheological characteristics and specific interactions in presence of mono- and divalent cations. From the depyruvylated variant Xan Δ L we conclude that the COO⁻-group of the terminal pyruvate ketal is mainly responsible for the increased viscosity and gel strength in presence of cations, while the combination of depyruvylation and higher degree of acetylation leads to dramatically decreased viscosity and gel strength. As pyruvate is known to decrease the ordered structural conformation of xanthan and a high degree of acetylation stabilizes the ordered structure, we conclude that the ordered, helical structure of xanthan results in a low viscosity and gel strength. Xan Δ L having the lowest viscosity and gel strength among all variants was therefore contributed to a synergistic effect of the absence of pyruvate and a higher degree of acetylation. By creating Xan Δ FL and Xan Δ GL with defined acetylation patterns in combination with the absence of the pyruvate ketal, it became evident that the inner mannose is more frequently acetylated than the outer mannose. While a higher degree of acetylation resulted in a decrease of viscosity, by linking the rheological properties of these variants to their acetylation pattern, we conclude that acetylation of the inner mannose is mainly responsible for stabilizing the ordered structure. Deacetylation at the specific mannose residues of Xan Δ F, Xan Δ G and Xan Δ FG led to a much lower degree of acetylation compared to the depyruvylated counterparts Xan Δ FL, Xan Δ GL and Xan Δ FGL and except for Xan Δ G their rheological properties were very similar to the unmodified xanthan. From the properties of Xan Δ G we concluded that only low degrees of acetylation of the inner mannose could stabilize ordered structure of xanthan enough to counter the destabilizing effect of the pyruvate ketal and therefore lead to an overall decreased viscosity. Effects of temperature on gel strength also showed that overall acetate content determines temperature stability, with higher acetate levels leading to a higher stability. Within this work, due to the nature of creating these xanthan-variants, we were able to directly link rheological properties to the distribution of acetate and pyruvate in the sidechain of xanthan to the rheological properties and gain several new insights on how these patterns affect the physicochemical behavior of xanthan. Additionally, this study shows that the rheological properties of the natural product xanthan can be specifically fine-tuned by modifying the acetylation and pyruvylation pattern on the genetic level towards defined and predictable properties for tailor-made applications. The question on how exactly

the substitution patterns affect the conformation of the sidechains and thereby the overall secondary structure of xanthan has yet to be investigated in detail.

Acknowledgements

We would like to acknowledge the Bavarian State ministry for Nutrition, Agriculture and Forestry (StMELF) for financing our research (project number N/16/06).

The plasmid pSRKGm was a friendly gift from Prof. Dr. Anke Becker, LOEWE Center for Synthetic Microbiology, Marburg.

Appendix A: Supplementary data

References

- Abbaszadeh, A., Lad, M., Janin, M., Morris, G., MacNaughtan, W., Sworn, G., & Foster, T. (2015). A novel approach to the determination of the pyruvate and acetate distribution in xanthan. *Food Hydrocolloids*, 44, 162-171.
- Becker, A., Katzen, F., Pühler, A., & Ielpi, L. (1998). Xanthan gum biosynthesis and application: a biochemical/genetic perspective. *Applied microbiology and biotechnology*, 50(2), 145-152.
- Bergmann, D., Furth, G., & Mayer, C. (2008). Binding of bivalent cations by xanthan in aqueous solution. *International Journal of Biological Macromolecules*, 43(3), 245-251.
- Bradshaw, I. J., Nisbet, B. A., Kerr, M. H., & Sutherland, I. W. (1983). Modified xanthan—its preparation and viscosity. *Carbohydrate Polymers*, 3(1), 23-38.
- Callet, F., Milas, M., & Rinaudo, M. (1987). Influence of acetyl and pyruvate contents on rheological properties of xanthan in dilute solution. *International Journal of Biological Macromolecules*, 9(5), 291-293.
- Candia, J. L. F., & Deckwer, W. D. (1999). Effect of the nitrogen source on pyruvate content and rheological properties of xanthan. *Biotechnology Progress*, 15(3), 446-452.
- Cheetham, N. W., & Norma, N. N. (1989). The effect of pyruvate on viscosity properties of xanthan. *Carbohydrate Polymers*, 10(1), 55-60.
- Dário, A. F., Hortêncio, L. M. A., Sierakowski, M. R., Neto, J. C. Q., & Petri, D. F. S. (2011). The effect of calcium salts on the viscosity and adsorption behavior of xanthan. *Carbohydrate Polymers*, 84(1), 669-676.
- Erten, T., Adams, G. G., Foster, T. J., & Harding, S. E. (2014). Comparative heterogeneity, molecular weights and viscosities of xanthans of different pyruvate and acetate content. *Food Hydrocolloids*, 42, 335-341.
- Galvan, E. M., Ielmini, M. V., Patel, Y. N., Bianco, M. I., Franceschini, E. A., Schneider, J. C., & Ielpi, L. (2013). Xanthan chain length is modulated by increasing the availability of the polysaccharide copolymerase protein GumC and the outer membrane polysaccharide export protein GumB. *Glycobiology*, 23(2), 259-272.
- Galván, Z. R. N., Soares, L. d. S., Medeiros, E. A. A., Soares, N. d. F. F., Ramos, A. M., Coimbra, J. S. d. R., & de Oliveira, E. B. (2018). Rheological Properties of Aqueous

- Dispersions of Xanthan Gum Containing Different Chloride Salts Are Impacted by both Sizes and Net Electric Charges of the Cations. *Food Biophysics*, 13(2), 186-197.
- García-Ochoa, F., Santos, V., Casas, J., & Gomez, E. (2000). Xanthan gum: production, recovery, and properties. *Biotechnology advances*, 18(7), 549-579.
- Hassler, R. A., & Doherty, D. H. (1990). Genetic engineering of polysaccharide structure: production of variants of xanthan gum in *Xanthomonas campestris*. *Biotechnology Progress*, 6(3), 182-187.
- Ielpi, L., Couso, R., & Dankert, M. (1981). Lipid-linked intermediates in the biosynthesis of xanthan gum. *FEBS letters*, 130(2), 253-256.
- Jansson, P.-E., Kenne, L., & Lindberg, B. (1975). Structure of the extracellular polysaccharide from *Xanthomonas campestris*. *Carbohydrate Research*, 45(1), 275-282.
- Katzen, F., Becker, A., Zorreguieta, A., Pühler, A., & Ielpi, L. (1996). Promoter analysis of the *Xanthomonas campestris* pv. *campestris* gum operon directing biosynthesis of the xanthan polysaccharide. *Journal of Bacteriology*, 178(14), 4313-4318.
- Kennedy, J. F., & Bradshaw, I. J. (1984). Production, properties and applications of xanthan. *Progress in Industrial Microbiology*, 19, 319-371.
- Khouryieh, H., Herald, T., Aramouni, F., Bean, S., & Alavi, S. (2007). Influence of deacetylation on the rheological properties of xanthan-guar interactions in dilute aqueous solutions. *Journal of food science*, 72(3).
- Kool, M. M., Gruppen, H., Sworn, G., & Schols, H. A. (2013). Comparison of xanthans by the relative abundance of its six constituent repeating units. *Carbohydrate Polymers*, 98(1), 914-921.
- Kool, M. M., Gruppen, H., Sworn, G., & Schols, H. A. (2014). The influence of the six constituent xanthan repeating units on the order-disorder transition of xanthan. *Carbohydrate Polymers*, 104, 94-100.
- Kool, M. M., Schols, H. A., Delahaije, R. J. B. M., Sworn, G., Wierenga, P. A., & Gruppen, H. (2013). The influence of the primary and secondary xanthan structure on the enzymatic hydrolysis of the xanthan backbone. *Carbohydrate Polymers*, 97(2), 368-375.
- Li, R., & Feke, D. L. (2015). Rheological and kinetic study of the ultrasonic degradation of xanthan gum in aqueous solution: effects of pyruvate group. *Carbohydrate Polymers*, 124, 216-221.
- Matsuda, Y., Biyajima, Y., & Sato, T. (2009). Thermal Denaturation, Renaturation, and Aggregation of a Double-Helical Polysaccharide Xanthan in Aqueous Solution. *Polymer Journal*, 41, 526.
- Milas, M., & Rinaudo, M. (1979). Conformational investigation on the bacterial polysaccharide xanthan. *Carbohydrate Research*, 76(1), 189-196.
- Palaniraj, A., & Jayaraman, V. (2011). Production, recovery and applications of xanthan gum by *Xanthomonas campestris*. *Journal of Food Engineering*, 106(1), 1-12.
- Rochefort, W. E., & Middleman, S. (1987). Rheology of Xanthan Gum: Salt, Temperature, and Strain Effects in Oscillatory and Steady Shear Experiments. *Journal of Rheology*, 31(4), 337-369.
- Rühmann, B., Schmid, J., & Sieber, V. (2014). Fast carbohydrate analysis via liquid chromatography coupled with ultra violet and electrospray ionization ion trap detection in 96-well format. *Journal of Chromatography A*, 1350, 44-50.
- Rüterling, M., Schmid, J., Rühmann, B., Schilling, M., & Sieber, V. (2016). Controlled production of polysaccharides—exploiting nutrient supply for levan and

- heteropolysaccharide formation in *Paenibacillus* sp. *Carbohydrate Polymers*, 148, 326-334.
- Sandford, P., Pittsley, J., Knutson, C., Watson, P., & Cadmus, M. (1977). Variation in *Xanthomonas campestris* NRRL B-1459: characterization of xanthan products of differing pyruvic acid content. *ACS Symposium Series-American Chemical Society (USA)*.
- Schmid, J., Huptas, C., & Wenning, M. (2016). Draft Genome Sequence of the Xanthan Producer *Xanthomonas campestris* LMG 8031. *Genome Announcements*, 4(5), e01069-01016.
- Schmid, J., Sieber, V., & Rehm, B. (2015). Bacterial exopolysaccharides: biosynthesis pathways and engineering strategies. *Frontiers in Microbiology*, 6(496).
- Shatwell, K. P., Sutherland, I. W., Dea, I. C., & Ross-Murphy, S. B. (1990). The influence of acetyl and pyruvate substituents on the helix-coil transition behaviour of xanthan. *Carbohydrate Research*, 206(1), 87-103.
- Smith, I., Symes, K., Lawson, C., & Morris, E. (1981). Influence of the pyruvate content of xanthan on macromolecular association in solution. *International Journal of Biological Macromolecules*, 3(2), 129-134.
- Tako, M., & Nakamura, S. (1984). Rheological Properties of Deacetylated Xanthan in Aqueous Media. *Agricultural and Biological Chemistry*, 48(12), 2987-2993.
- Tako, M., & Nakamura, S. (1988). Rheological Properties of Depyruvated Xanthan in Aqueous Media. *Agricultural and Biological Chemistry*, 52(6), 1585-1586.
- Vorhölter, F. J., Schneiker, S., Goesmann, A., Krause, L., & Bekel, T. (2008). The genome of *Xanthomonas campestris* pv. *campestris* B100 and its use for the reconstruction of metabolic pathways involved in xanthan biosynthesis. *Journal of Biotechnology*, 134(1-2), 33-45.
- Wang, X., Zheng, D., & Liang, R. (2016). An Efficient Electro-Competent Cells Generation Method of *Xanthomonas campestris* pv. *campestris*: Its Application for Plasmid Transformation and Gene Replacement. *Advances in Microbiology*, 6(02), 79.
- Wu, M., Qu, J., Shen, Y., Dai, X., Wei, W., Shi, Z., Ma, T. (2018). Gel properties of xanthan containing a single repeating unit with saturated pyruvate produced by an engineered *Xanthomonas campestris* CGMCC 15155. *Food Hydrocolloids*, 87, 747-757.
- Xu, L., Dong, M., Gong, H., Sun, M., & Li, Y. (2015). Effects of inorganic cations on the rheology of aqueous welan, xanthan, gellan solutions and their mixtures. *Carbohydrate Polymers*, 121, 147-154.